Properties of Small Metallic Particles

Helen Chappell, Aikaterina Plati, Yi Shen **18th December 2002**

Supervisors: Professor Harry Bhadeshia, Dr Thomas Sourmail

Phase Transformations and Complex Properties Research Group, Department of Materials Science and Metallurgy, University of Cambridge.

1.Introduction

Small particles have long been studied in metallurgy because many properties, such as melting temperature, depend on particle size. With the advent of new nanotechnologies, the study of such particles has become even more relevant.
This project has involved modelling the effects on melting temperature with respect to changes in particle size, shape, crystal structure and chemical composition.

Using a sketch of temperature against Gibbs free energy, the melting temperature of a solid, T_m, can be found from plotting a line for G_S, the Gibbs free energy of the solid, and a line for G_L, the Gibbs free energy of the liquid; their intersection giving the melting temperature of the solid. That is, for a flat interface at T_m,

$$G_L = G_S \qquad \textbf{(1)}$$

However, for the curved interface of a small particle, the melting temperature is reduced. For this case, at T_{mr},

$$G_L = G_S + \sigma\, ds/dn \qquad \textbf{(2)}$$

where ds/dn is the increase in surface are per atom added and σ the interfacial energy. This surface area depends on the shape of the particle. This is illustrated in Figure 1.

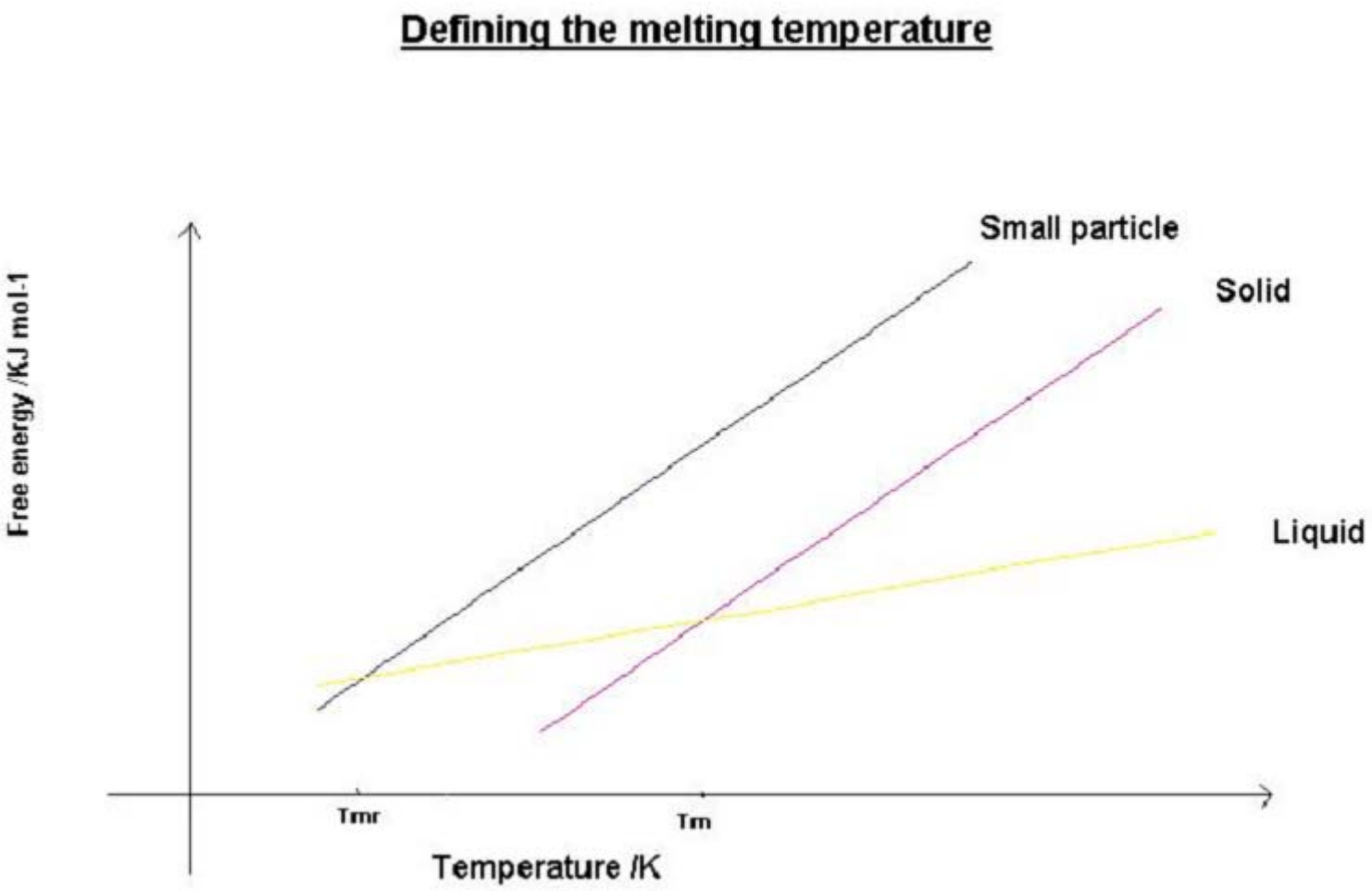

Figure 1. Defining the melting temperature of solid and small particles

In order to investigate these variations in melting temperature, the project was organised into three parts.

1. The first part of the project involved the modelling of pure iron particles. Calculations of melting temperatures were carried out for both spherical and cylindrical particles and this was done for both a face-centred cubic structure

(austenite) and a body-centred cubic structure (ferrite). For these four different sets of conditions, particle radius was varied from 1×10^{-9} m to 1×10^{-7} m and the new melting temperatures recorded.

2. The second part of the project involved modelling these same variations in melting temperature, but this time for the ferritic and austenitic phases of iron in a nickel-iron alloy of 10-wt% nickel, for the case where both liquid and solid have identical composition.

3. The third part of the project involved a statistical analysis of the composition of a sample of atoms taken from a fixed volume of the 10-wt% nickel- iron alloy. This analysis allowed a distribution of melting temperatures as a function of particle radius to be created. That is, for any random sample of atoms chosen from a fixed volume of known composition, a distribution of melting temperatures was created based on the statistical probability of the composition of that chosen sample.

2.Nomenclature

G_L - Gibbs free energy of liquid phase

G_S - Gibbs free energy of solid phase

G_{SR} – Gibbs free energy of small particle phase

T_m – melting temperature

T_{mr} – revised melting temperature with small particles

r – radius of particle

V_m – molar volume of solid

σ – interfacial energy per unit area

N – Avogadro's number (6.022×10^{23} mol $^{-1}$)

a – lattice parameter

α – thermal expansion coefficient

l_0 – length of cell parameter at 273K

l_t - transformed length of cell parameter at given temperature

N_a – number of atoms in a particle

N_p - number of particles

f – probability of finding a nickel atom in a given sample of a nickel-iron alloy

3.Materials and Methods

3.1 MTDATA

The thermodynamic calculations were all carried out using a commercially available software package and database. MTDATA is a software package, first created in 1970 at the National Physical Laboratory. It contains a vast amount of critically assessed thermodynamic data that can be used in the calculation of phase equilibria in multiphase and multicomponent systems [1,2]. The program minimises the Gibbs free energy of a system, thereby calculating the equilibrium composition and volume fractions of the phases present. Any phase may be suppressed in these calculations and the calculations re-run.

The thermodynamic data needed to do this are found in the SGTE database. For larger systems where data are not available thermodynamic theory is used to make predictions. Although this program can give extremely useful data it says nothing of the kinetics of phase formation [3]. This package was used in all three parts of the project to find Gibbs free energy values at varying temperatures. Table 1 shows the phases for which these data were collected.

Phase	**Iron**	**Nickel-Iron Alloy**
BCC_A1 ferrite	G_S	G_S
FCC_A2 austenite	G_S	G_S
Liquid	G_L	G_L

Table 1. Data retrieved from MTDATA

These calculations were run for one mole of the given substance, with temperature ranging from 573–1973 K, stepped by two-Kelvin intervals.

3.2 Excel

The Excel statistical package was used to create graphs of the figures obtained from MTDATA, and to fit polynomial equations to these data. These equations were then used for the calculation of melting temperature as a function of particle radius, as described in Section 1, using the Curvefit3 program developed in this project.

3.3 Curvefit3

Curvefit3 is a program written in FORTRAN 77 to find the melting temperature of particles of different radii, which have a fixed composition. These data were again transferred to Excel files so plots of particle radii against melting temperature for a given interfacial energy value, could be generated. Figure 2 shows a flow diagram explaining the function of this program. The program transcript is given in Appendix 1.

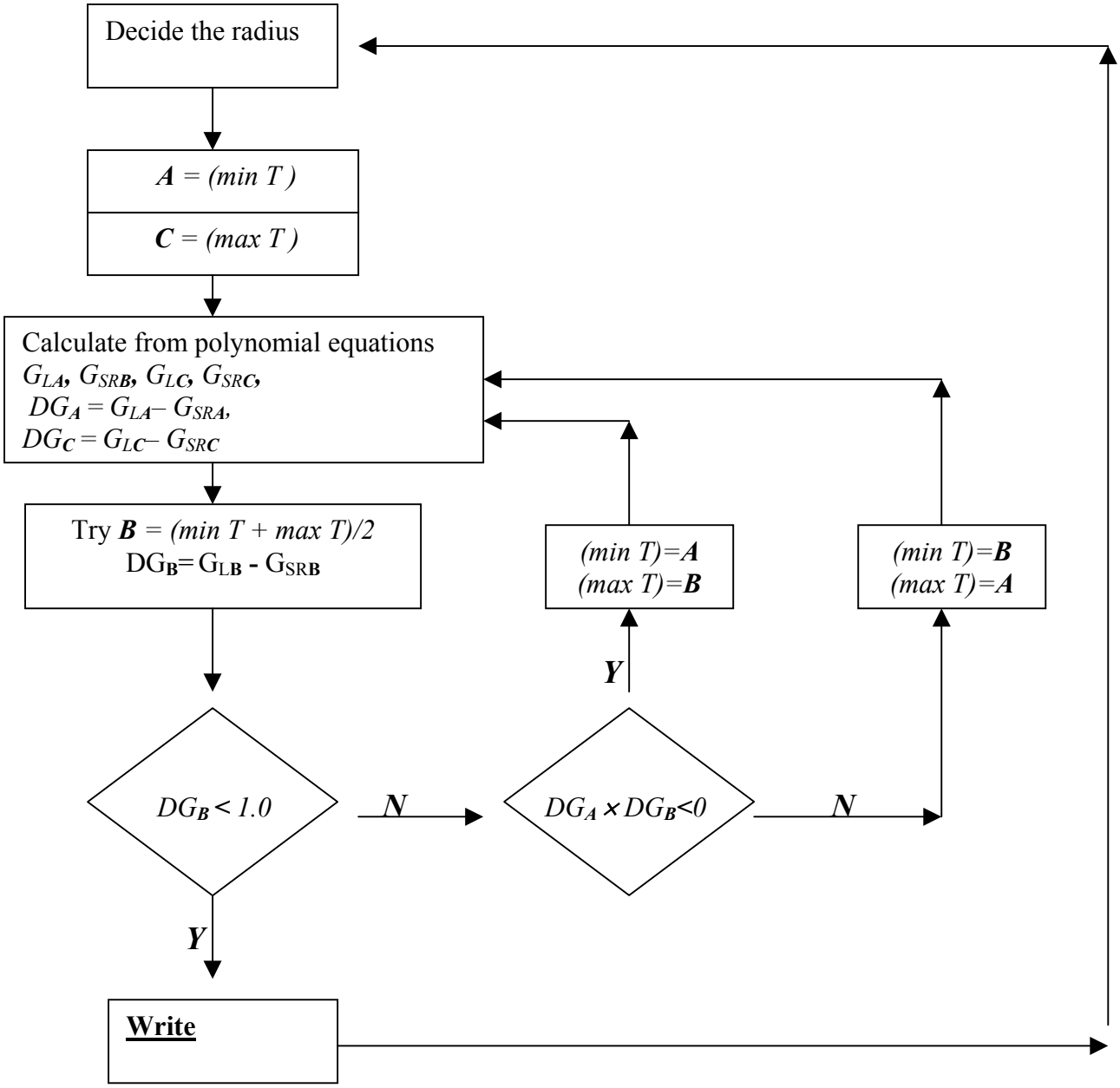

Figure2. Flowchart for Curvefit3

3.4 Try

Try is a program written for this project in FORTRAN 77 [4]. This program was used for the third part of the project. It finds the range of possible compositions for a specific number of atoms taken from a sample of fixed composition and fixed volume. It then tabulates these compositions with melting temperature. The results are produced in the form of sample radius against melting temperature. This program allowed for different values of σ and different compositions to be specified. For our specific calculations, using the nickel-iron alloy, a fixed composition of 10-wt% nickel was used and the value of σ was varied from 0.1 to 0.5 Jm^{-2}. Figure 3 shows a flow diagram explaining the function of this program. The program transcript is given in Appendix 1.

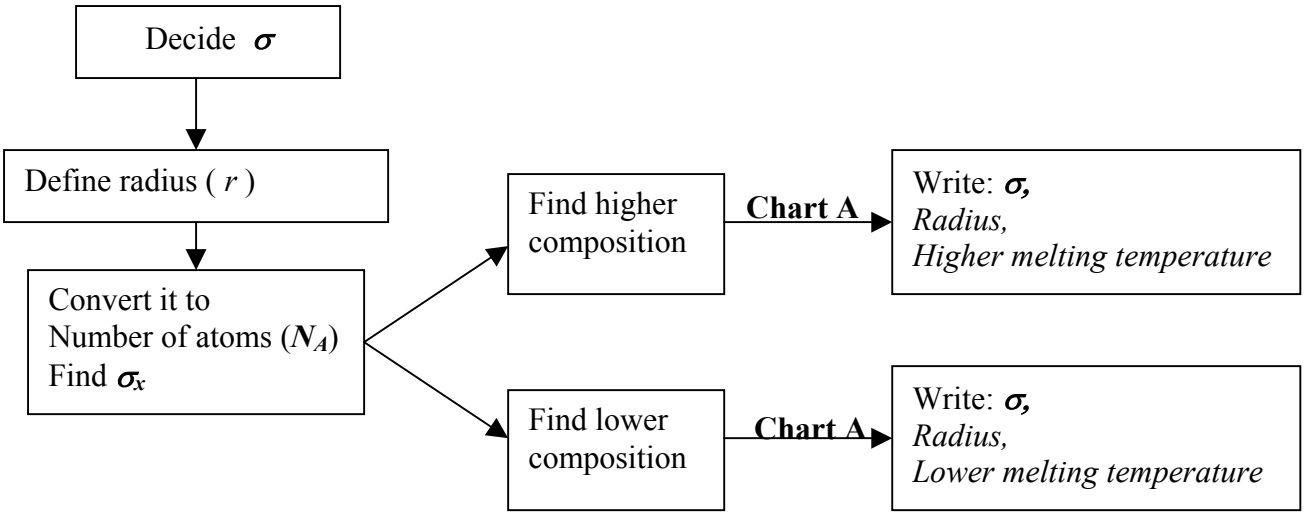

Chart A

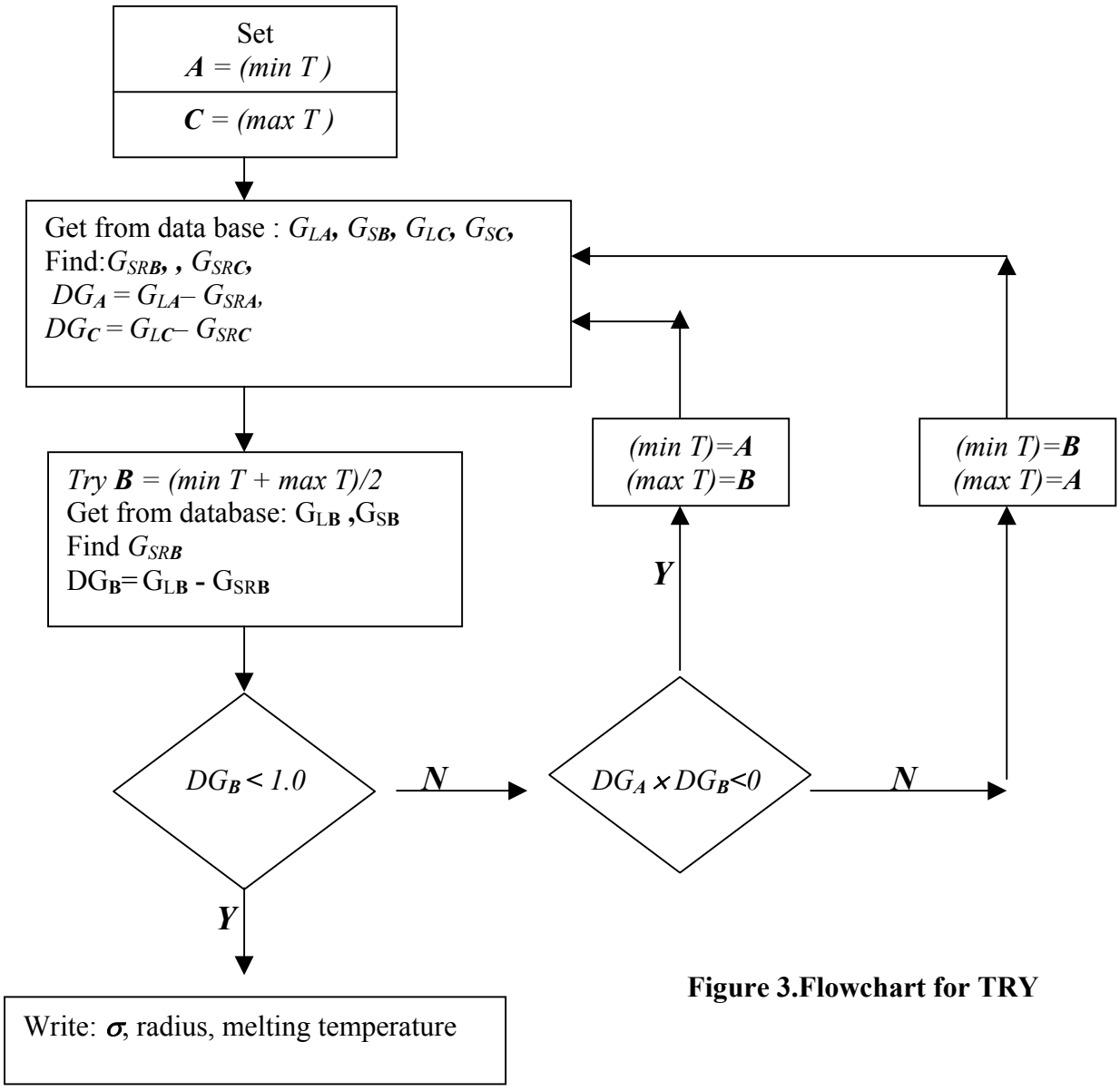

Figure 3.Flowchart for TRY

4.Results and Discussion

4.1 Iron Particles

For the data collected from MTDATA for this system, it was found that second order polynomial equations made the best fit with correlation coefficients of $R = 1$. These equations are given in Table 2.

G_S (kJ/mol)– ferrite	G_S (kJ/mol) – austenite	G_L(kJ/mol)
$y = -0.0176T^2 – 31.274T + 6207.5$	$y = -0.014T^2 – 41.2827T + 13818$	$y = -0.0146T^2 – 47.827T + 26339$

Table 2. Polynomial equations for iron data, where *T* is temperature

As is discussed in Section 1,

$$G_{SR} = G_S + \sigma\, ds/dn \quad \textbf{(3)}$$

For a spherical particle, ds/dn is given by $2V_m/r$, where V_m is the molar volume and r the radius of the particle. Thus, G_{SR}, the Gibbs free energy of the particle phase, is given by,

$$G_{SR} = G_S + \sigma\, 2V_m/r \quad \textbf{(4)}$$

$2V_m/r$ is derived as follows:

$$dV = dnV_m,$$

where V is particle volume.

Therefore, $dn = dV/V_m$

$$V = 4/3\pi r^3$$

Therefore, $dV/dr = 4\pi r^2$

and, $dV = 4\pi r^2.dr$

Thus, $dn = 4\pi r^2.dr/ V_m$

Surface area, $s = 4\pi r^2$

Therefore, $ds/dr = 8\pi r$

and $ds = 8\pi r.dr$

$$ds/dn = 8\pi r.dr/ 4\pi r^2.dr/ V_m = 2V_m/r$$

For an infinite cylindrical particle the value of ds/dn is V_m/r. This assumes the surface area is solely the curved surface of the cylinder. This equation can be derived in exactly the same manner as equation **(4)**. This gives equation **(5)**.

$$G_{SR} = G_S + \sigma V_m/r \qquad \textbf{(5)}$$

V_m, the molar volume, can be derived easily from the cube of the lattice parameter which itself has a temperature dependence. Therefore the lattice parameter is given by,

$$a_t = a + (1+\alpha T) \qquad \textbf{(6)}$$

where a_t is the revised lattice parameter, a the original lattice parameter and α the expansion coefficient.

Therefore,

$$V_m = (a + (1+\alpha T))^3 \times N /2 \quad \text{for the ferrite structure} \quad \textbf{(7)}$$

where N is Avogadro's Number.

and,

$$V_m = (a + (1+\alpha T))^3 \times N/4 \quad \text{for the austenite structure} \quad \textbf{(8)}$$

Values for a were taken from [4]. Table 3 gives the equations for G_{SR} for both spherical and cylindrical particles of the austenite structure and the ferrite structure.

	Ferrite	**Austenite**
Spherical particles	$G_{SR}\,(\text{kJ/mol}) = G_s + \sigma(2\times (a + (1+1.18e-6T))^3 \times N/2)/r$	$G_{SR}\,(\text{kJ/mol}) = G_s + \sigma(2\times (a + (1+1.8e-6T))^3 \times N/4)/r$
Cylindrical particles	$G_{SR}\,(\text{kJ/mol}) = G_s + \sigma\times (a + (1+1.18e-6T))^3 \times N/2)/r$	$G_{SR}\,(\text{kJ/mol}) = G_s + \sigma\times (a + (1+1.8e-6T))^3 \times N/4)/r$

Table 3. G_{SR} equations for iron particles

Using these equations in Curvefit3, the following results were generated. Figure 4 shows the results for ferritic spherical particles, Figure 5 the results for austenitic spherical particles, Figure 6 the results for ferritic cylindrical particles and Figure 7 the results for austenitic cylindrical particles. All these plots have been constructed with *1/r* on the x-axis for clarity.

The first thing to note in these results is the maximum melting temperatures for the two different compositions. Looking at Figures 4 and 5 it can be seen that the maximum melting temperature for the ferrite structure is 1811.45 K but this temperature is reduced by approximately 150 K to 1661.41 K in the austenite structure. This observation can be explained be reference to the density of the two crystal structures. The ferrite structure, unlike that of the austenite, is not close packed. This structure is thus less dense. The effect of this reduced density is an increased entropy term at higher temperature, which reduces the Gibbs free energy. Therefore, the ferrite structure is stable to higher temperatures than the austenite [6].

It is also true that the austenite structure has a broader range of melting temperatures, 1548.63 K separating the highest and lowest temperatures, compared to a difference of just 1419.57 K for the ferrite structure.

The charts are plotted such that each line represents the use of a different interfacial energy value. In all cases, the larger this value the lower the melting temperature. This observation is true for both spherical and cylindrical particles.

The reason for this is that the value of G_{SR} would be made less negative as the additional Gibbs energy given by *ds/dn* is a positive quantity. Because the Gibbs energy of the system is increased for a given temperature, the melting temperature will decrease in order to minimise the energy of the system. That is, the liquid phase has a lower Gibbs energy than the particle phase at higher temperatures.

Additionally, *ds/dn* is increased by decreasing the radius of the particle, as is evident from equation **(4)**. Thus, once again, the Gibbs free energy is increased and the melting temperature is reduced. This is true for both spherical and cylindrical particles.

Turning to Figures 6 and 7, the most obvious observation is the decreased range of melting temperatures. For example, the difference in T_{mr} at its greatest (i.e. the smallest radius) is just 817.01 K for the austenitic cylindrical particles. This compares to a range of 1548.63 K for the spherical particles. Naturally, this is a consequence of the factor of 2, which is missing from equation **(5)**, as compared to equation **(4)**. This shows that the spherical particle maximises the curved interface for a particle of a given radius.

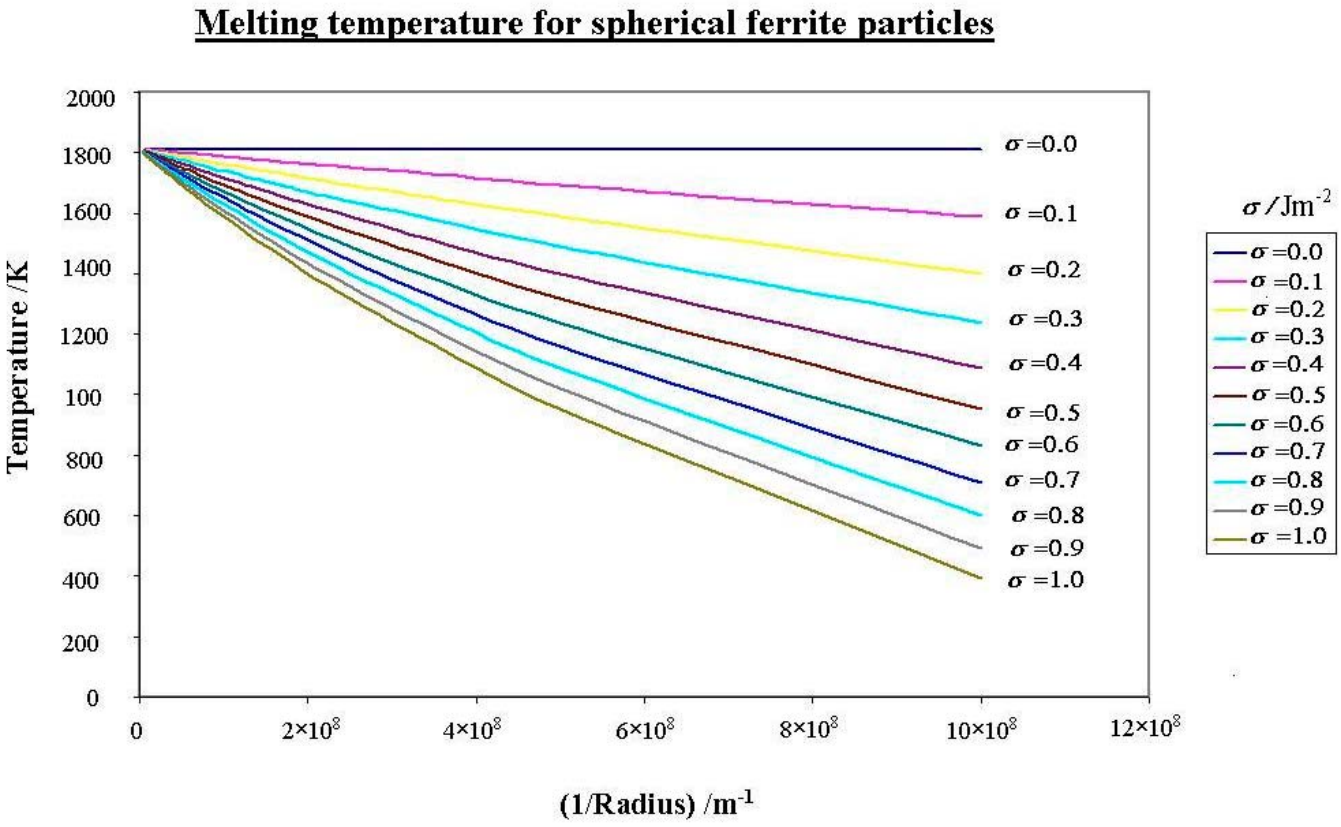

Figure 4. Spherical ferrite particles in iron

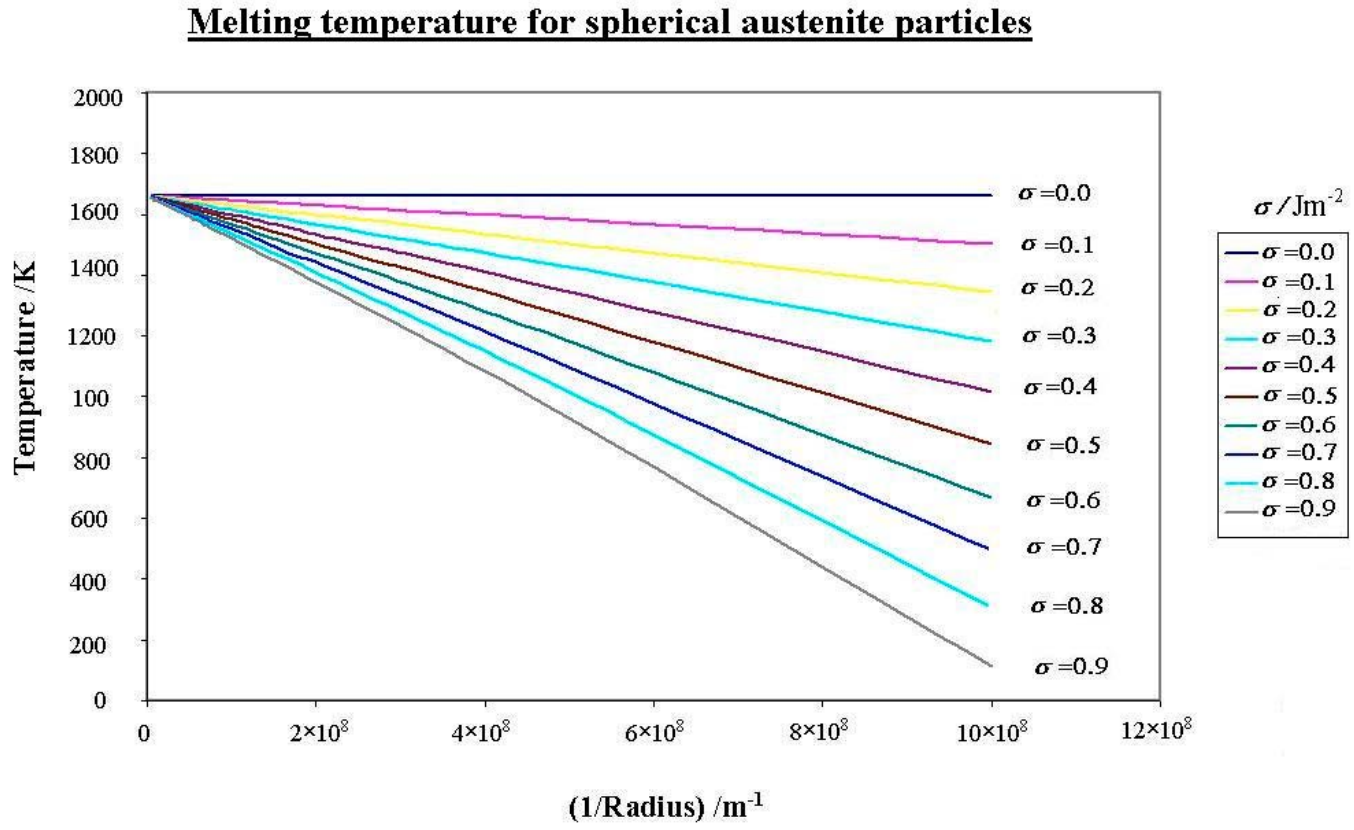

Figure 5. Spherical austenite particles in iron

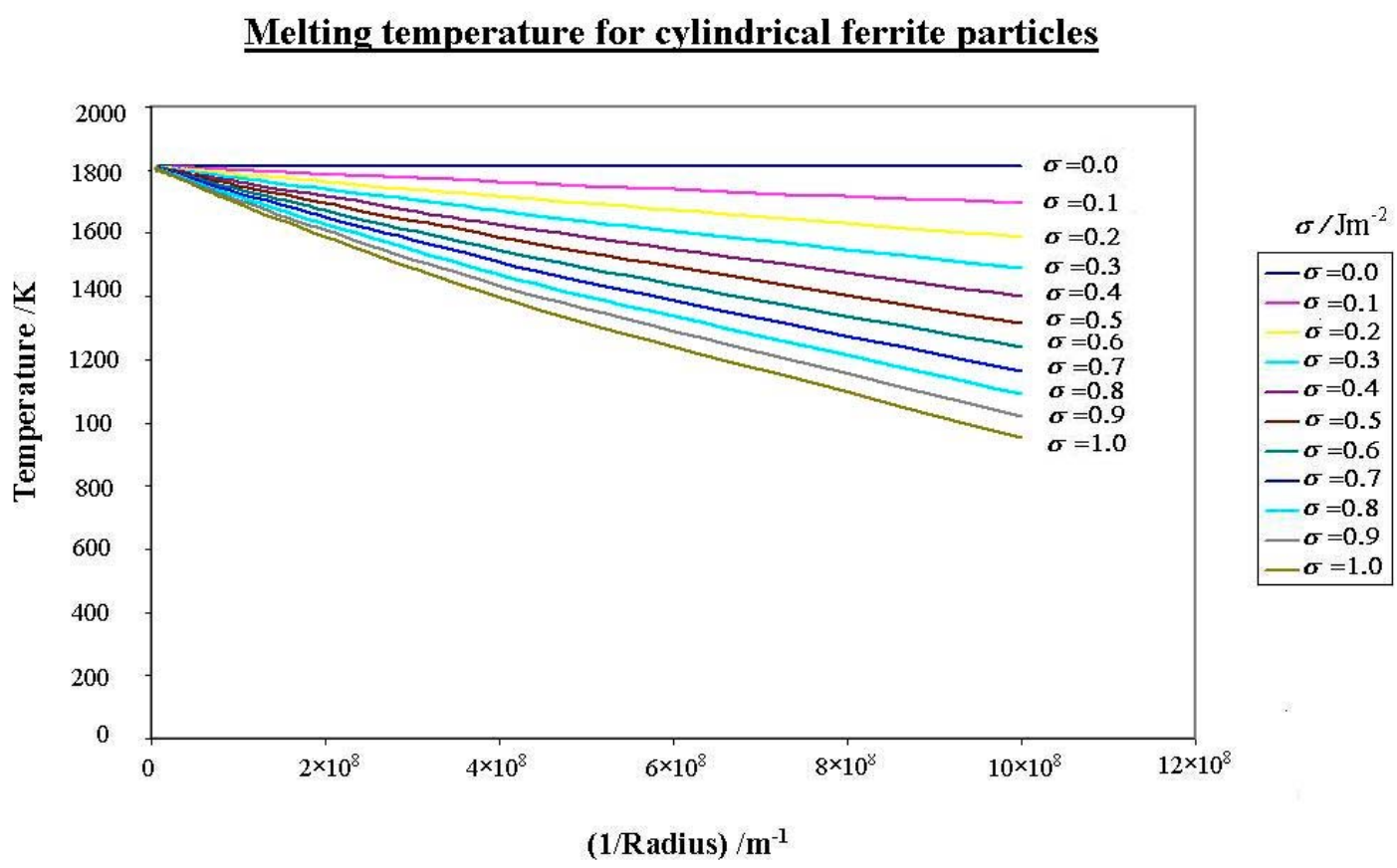

Figure 6.Cylindrical ferrite particles in iron

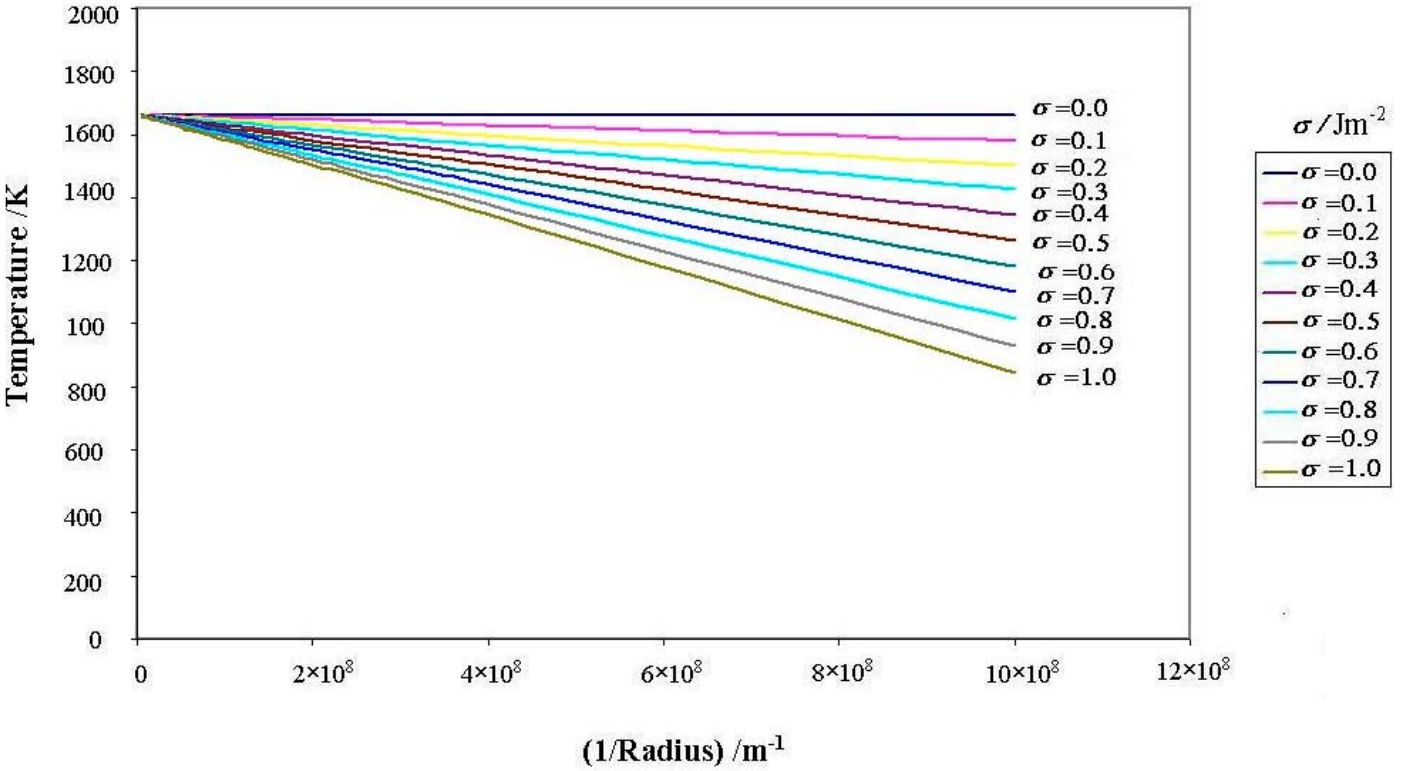

Figure 7. Cylindrical austenite particles in iron

4.2 Nickel-Iron Alloy Particles

The same analysis was carried out with a 10-wt% nickel-iron alloy. For the data collected from MTDATA , it was again found that second order polynomial equations made the best fit, with the *R* value equal to 1. These equations are given in Table 4.

G_S (kJ/mol) – ferrite	G_S (kJ/mol) – austenite	G_L (kJ/mol)
$y = -0.0172T^2 - 35.564T + 7602.5$	$y = -0.0141T^2 - 44.14T + 12886$	$y = -0.0146T^2 - 50.209T + 25307$

Table 4. Polynomial equations for alloy data, where *T* is temperature

The G_{SR} equations are the same as those for the iron particles, as given in Table 3.

Curvefit3 produced the following results. Figure 8 shows the results for ferritic spherical particles, Figure 9 the results for austenitic spherical particles, Figure 10 the results for ferritic cylindrical particles and Figure 11 the results for austenitic cylindrical particles.

The first thing to note here is that the melting temperature for $\sigma = 0.0$ Jm^{-2} in the alloy, is higher for the austenite crystal structure than for the ferrite crystal structure as can be seen on Figures 8 and 9. The difference is small with an austenite T_m of 1784.3 K and a ferrite T_m of 1756.84 K. This is in contrast to a pure iron sample where the austenite structure has a much lower T_m value. This occurs because the nickel atoms in the structure stabilize the austenitic form relative to the ferritic form. However, despite this difference, the austenite structure, as with pure iron, has a broader range of melting temperatures than the ferrite structure. Comparing the range

from $\sigma = 0.0 - 0.9$ Jm^{-2} in spherical particles, austenite has a T_m range spanning 1679.05 K and ferrite a range spanning 1391.12 K.

However, for the cylinders, the two ranges are almost the same, the austenite range spanning 897.69 K and the ferrite range spanning 856.75 K.

For the alloy particles, the same trends have been observed as for the iron; calculations using larger interfacial energies and smaller radii giving lower melting temperatures. Again, this would be expected because of the increase in Gibbs free energy.

Figure 12 shows a comparison between iron and nickel-iron alloy particles at a $\sigma - value$ of 0.5 Jm^{-2}. This figure clearly illustrates the differences between the two; the austenite particles in the alloy being less stable than the austenite particles in the iron and the spherical particles less stable than the cylindrical particles.

One interesting observation that can be seen for both the iron particles and the alloy particles is the curvature of the plotted lines. In all cases the lines plotted for the austenite data curve downwards whilst all the lines plotted for the ferrite data, curve upwards. This is most pronounced for the spherical particles in Figures 8 and 9. The reason for this has yet to be determined.

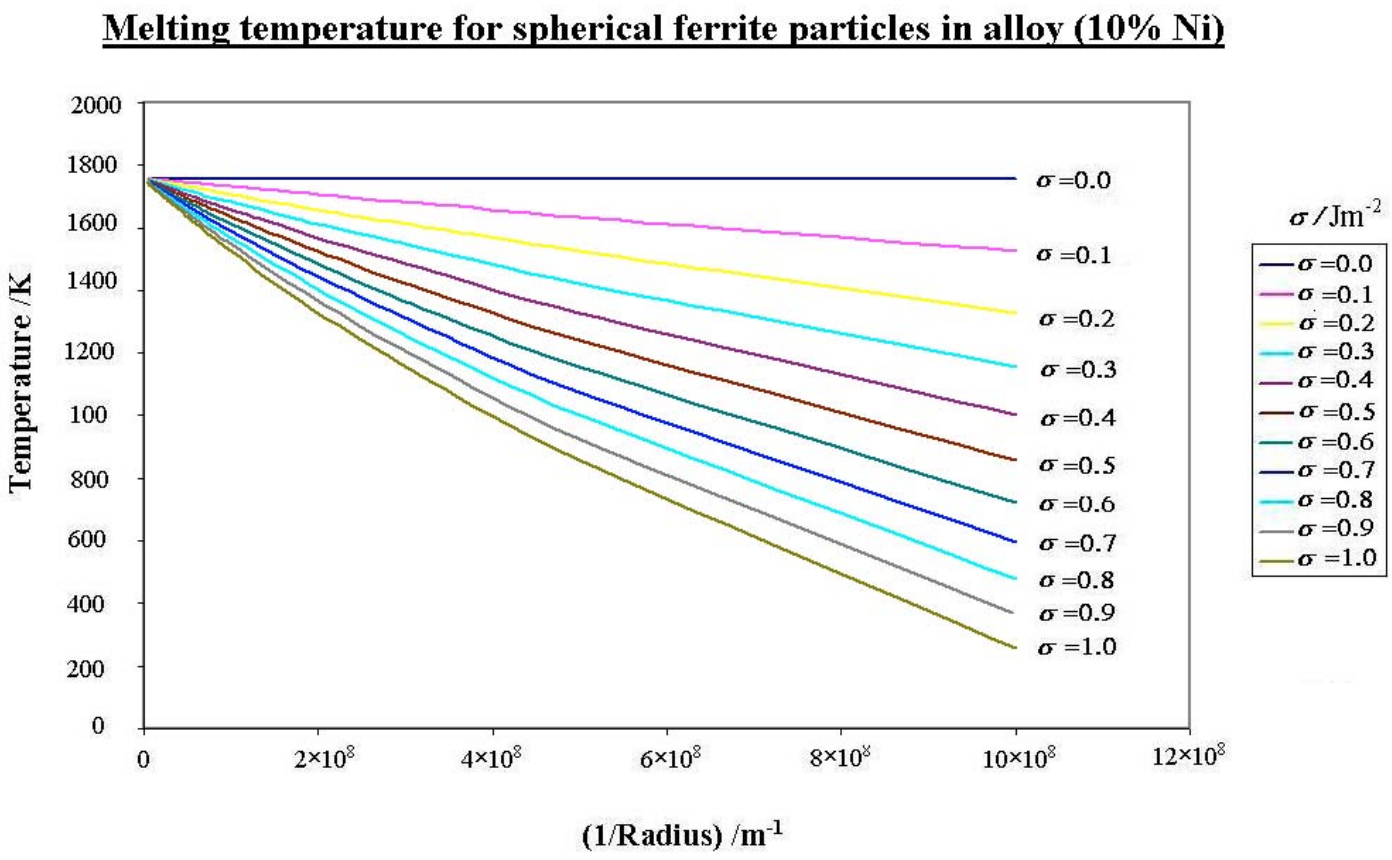

Figure 8. Spherical ferrite particles in 10-w% nickel-iron alloy

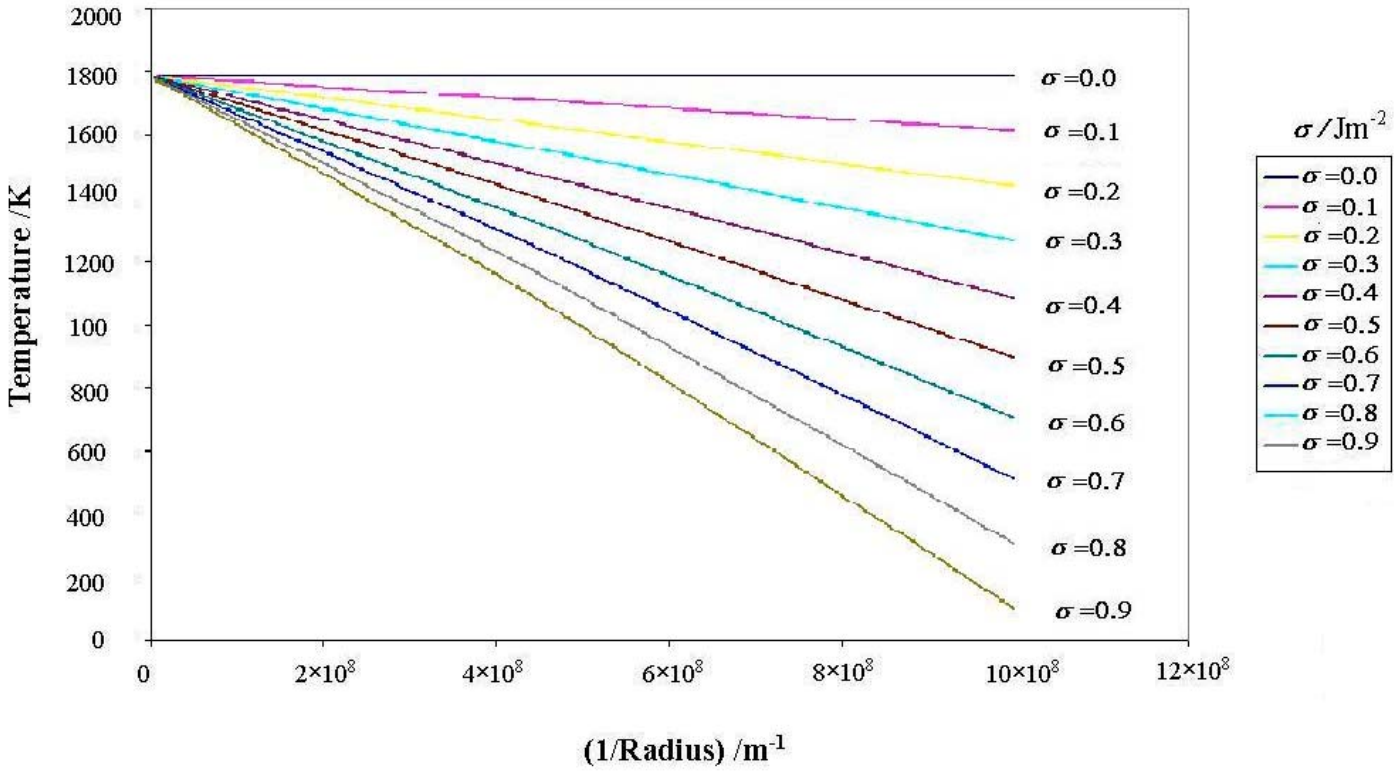

Figure 9. Spherical austenite particles in 10-wt% nickel-iron alloy

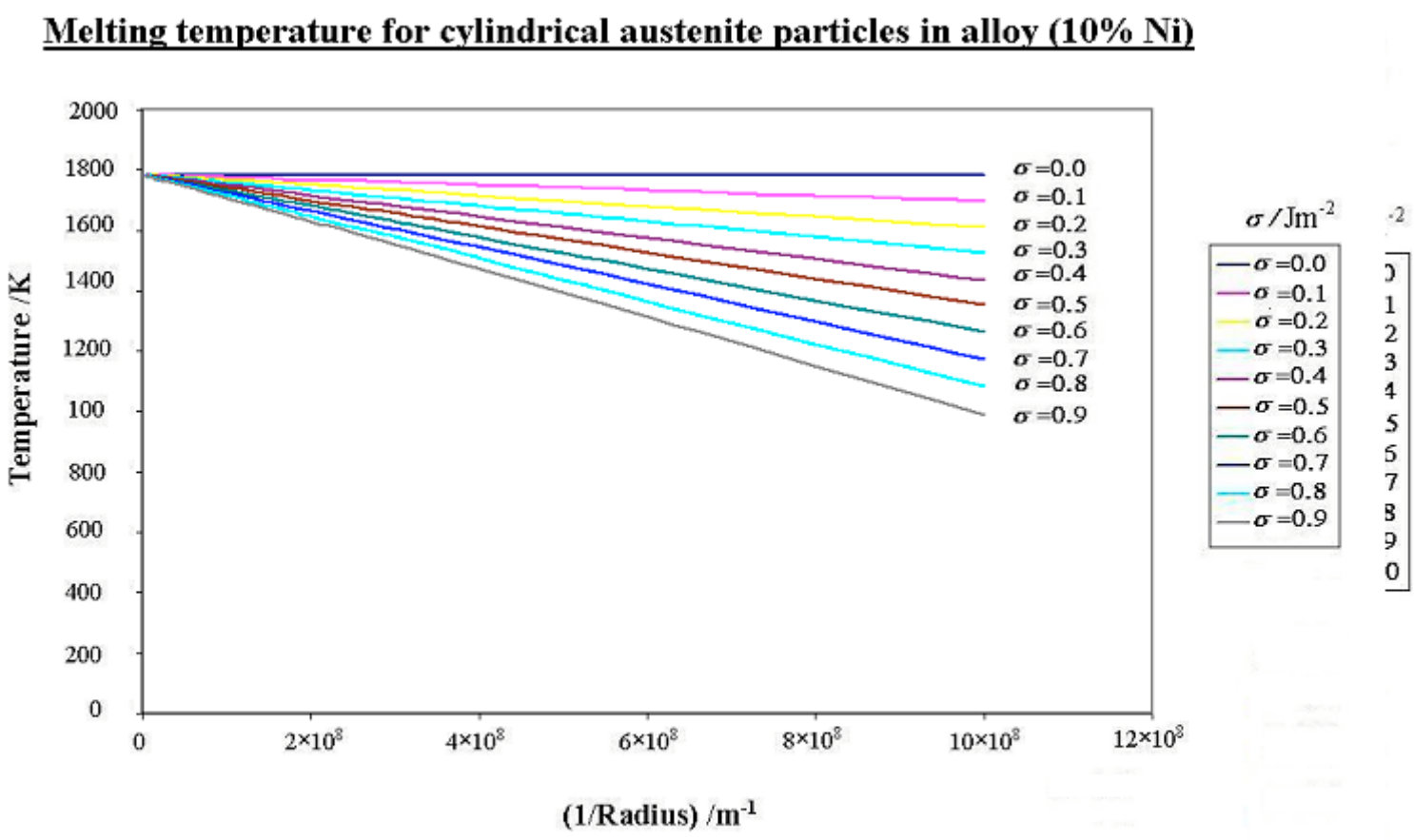

Figure 10 Cylindrical ferrite particles in 10-wt% nickel-iron alloy

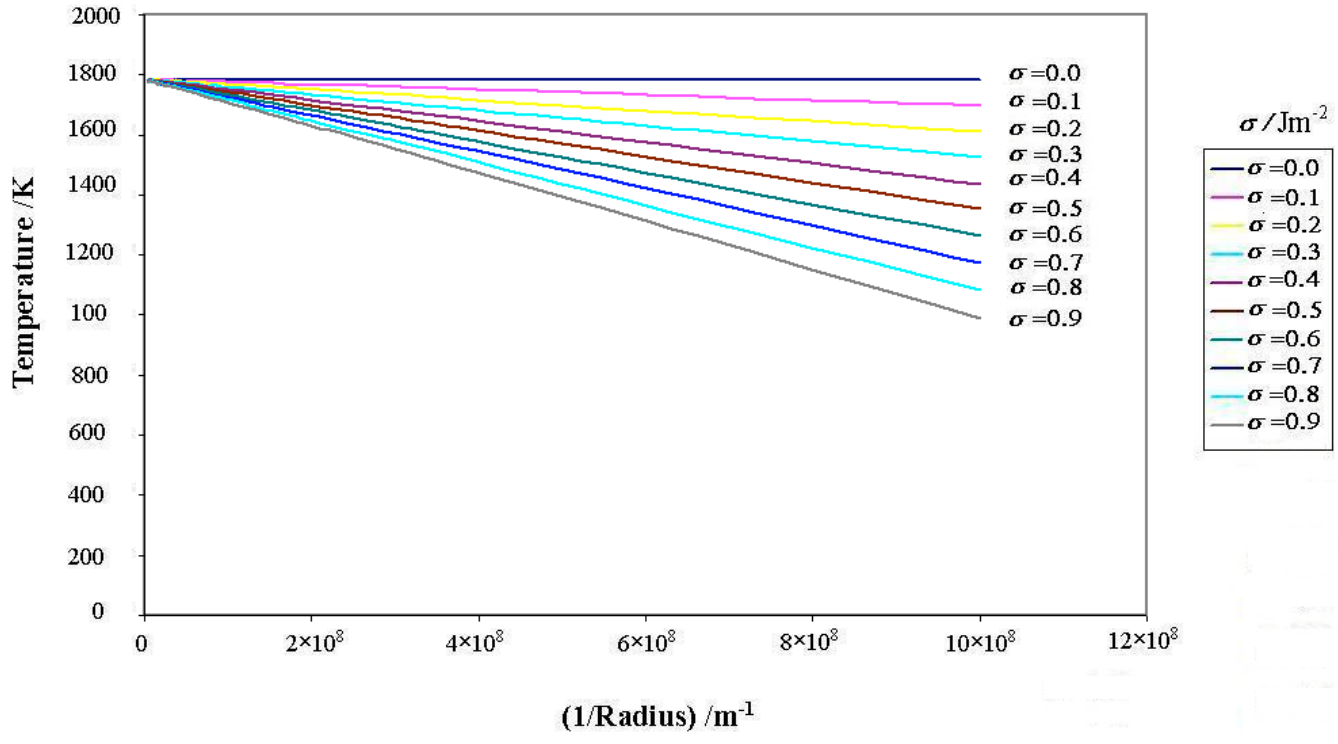

Figure 11.Cylindrical austenite particles in 10-wt% nickel-iron alloy

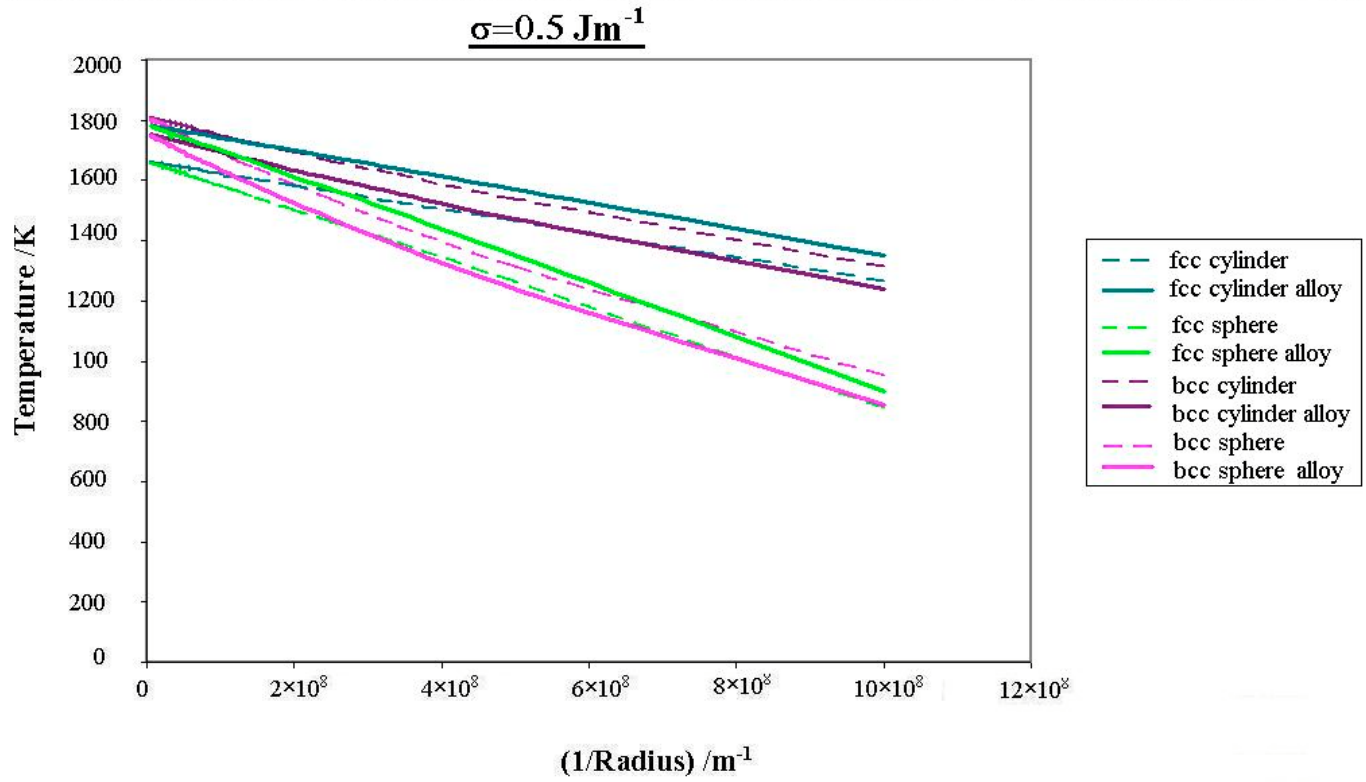

Figure 12. Comparison of melting temperatures of austenite and ferrite particles

4.3 Statistical Analysis of Composition and Melting Temperature

For this part of the project a 10-wt% nickel-iron alloy was used in the calculations. It was assumed that the volume of our sample from which a particle of a given radius would be picked, would remain constant. That is,

$$N_p \times N_a = constant$$

where N_p is the number of particles and N_a is the number of atoms.

For this fixed composition, the distribution, showing the fractional composition of nickel within a chosen sample will be binomial and the standard deviation will therefore be,

$$\sigma_x = \sqrt{N_a \times f(1-f)} \qquad \textbf{(9)}$$

where σ_x is the standard deviation and f the probability of finding a nickel atom in a given sample of nickel-iron alloy.

Thus the fractional composition of nickel in a particle will be between $0.1 + \sigma_x$ and $0.1 - \sigma_x$. N_a in equation **(9)** is given by equation **(10)**.

$$N_a = (4/3\pi r^3)/ V_m \times N \qquad \textbf{(10)}$$

Equation **(10)** allows the composition of a particle to be found simply from the radius of that particle. Therefore, the TRY program was used to find these distributions of composition, as given by the radius of the sample particle and this was correlated with the corresponding melting temperatures. It was then possible to plot radius against melting temperature. This gave two lines, one corresponding to the maximum nickel

composition and one corresponding to the minimum nickel composition for a given radius. The true melting temperature would probably lie somewhere in between these two. Figure 13 shows these results for a fixed composition of 10-wt% nickel, varying the interfacial energy, σ, from 0.1 to 0.5 Jm^{-2}.

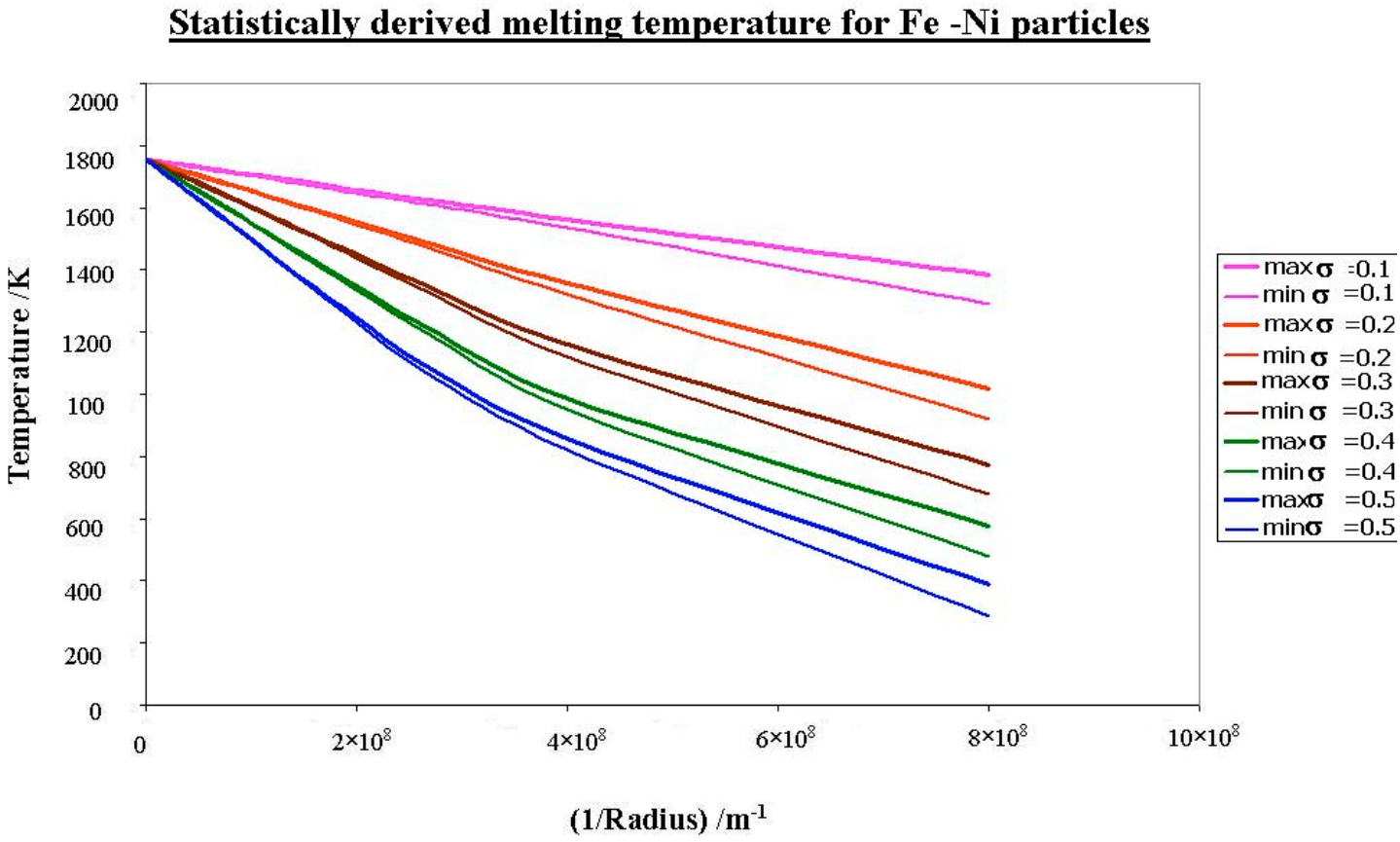

Figure 13.Statistically derived melting temperature for particles of 10 -wt% nickel - iron alloy

These results show that there is only a significant difference in melting temperatures between the maximum and minimum nickel composition when the radius of the particle is extremely small. Any particle with a radius greater than approximately 2×10^{-8} m will essentially have a constant melting temperature. Only for very small sample sizes is the compositional uncertainty of consequence.

5. Conclusion

During the course of this project a number of interesting observations were recorded. Firstly, it is evident that spherical particles have the greatest effect on melting temperature of a sample. This indicates that the sphere maximises the curved surface interface. Cylindrical particles also reduce the melting temperature but to a lesser extent.

Secondly, the factors that decrease the melting temperature are 1) an increase in interfacial energy and 2) a decrease in particle radius. Thus, the lowest melting temperatures are found with extremely small particles and a large interfacial energy. For the 10-wt% nickel-iron alloy, the same effects are observed but the reduction in melting temperature spans a narrower range than for the pure iron particles.

The third part of the project revealed that the melting temperature of a sample particle would be practically constant except for extremely small particles of less than 2×10^{-8} m.

Hopefully, these results will be used in future research.

6.Acknowledgments

With thanks to Harry. Aussi, un grand merci à Thomas pour son aide, sa patience et surtout, pour ses chocolats!

7. References

1. http://www.npl.co.uk/npl/cmmt/mtdata/mtdata.html
2. Davies R H, Dinsdale A T, Hodson S M, Gisby J A, Pugh N J, Barry T I, Chart T G, *Proc. Conf. "User Aspects of Phase Diagrams"*, 25-27 June 1990, Petten, Institute of Metals. **"MTDATA - The NPL databank for metallurgical thermochemistry"**.
3. Yescas Gonzalez, M.A. (2001). **Modelling the Properties of Austempered Ductile Cast Iron**. **Pages 109-110**. University of Cambridge.
4. Thomas Sourmail. (2002). **Try**.
5. www.liv.ac.uk/~goodhew/CubicStructures_Hout.doc
6. Cottrell, A. (1988). Introduction To The Modern Theory of Metals. Institute of Metals.

8. Appendix 1

8.1 Curvefit3

```
      PROGRAM CURVEFIT
      implicit none
      INTEGER I,J
      DOUBLE PRECISION VCELL,AVOGA
      DOUBLE PRECISION RADIUS,TEMPA,GS,GL,GSR,TEMPB,TEMPC
      DOUBLE PRECISION GSA,GSB,GSC,GLA,GLB,GLC,GSRA,GSRB,GSRC
      DOUBLE PRECISION DGA,DGB,DGC,VCELLA,VCELLB,VCELLC
      DOUBLE PRECISION SIGMA,DEPS

      WRITE(*,*)
      WRITE(*,*) "Enter sigma:"
      READ(*,*) SIGMA
      AVOGA=6.0221E23
      DEPS=1.0
      DO 10 I=1,200
         TEMPA=0.0
         TEMPB=1973.0
 3       TEMPC=(TEMPA+TEMPB)/2
c         WRITE(*,*) TEMPC
         RADIUS=DBLE(I)*1e-09
         GSA=-0.0172*(TEMPA**2)-35.564*TEMPA+7602.5
         GSB=-0.0172*(TEMPB**2)-35.564*TEMPB+7602.5
         GSC=-0.0172*(TEMPC**2)-35.564*TEMPC+7602.5
         GLA=-0.0146*(TEMPA**2)-50.209*TEMPA+25307
         GLB=-0.0146*(TEMPB**2)-50.209*TEMPB+25307
         GLC=-0.0146*(TEMPC**2)-50.209*TEMPC+25307
         VCELLA=(2.86E-10*(1+(1.18E-6)*TEMPA))**3
         VCELLB=(2.86E-10*(1+(1.18E-6)*TEMPB))**3
         VCELLC=(2.86E-10*(1+(1.18E-6)*TEMPC))**3
         GSRA=GSA+(SIGMA*(VCELLA*AVOGA/2.)/RADIUS)
         GSRB=GSB+(SIGMA*(VCELLB*AVOGA/2.)/RADIUS)
         GSRC=GSC+(SIGMA*(VCELLC*AVOGA/2.)/RADIUS)
         DGA=GLA-GSRA
         DGB=GLB-GSRB

         DGC=GLC-GSRC
c         WRITE(*,*) DGA,DGC,DGB
         IF ((DGA*DGC).lt.0) then
            TEMPA=TEMPA
            TEMPB=TEMPC
         ELSE
            TEMPA=TEMPC
            TEMPB=TEMPB
         ENDIF
         IF (DABS(DGB).GT.DEPS) GOTO 3
 5       write(*,100) RADIUS,TEMPC,GSC,GSRC,GLC
 10   continue

 100  FORMAT(E12.6,4(1x,E12.6))

      end
```

8.2 TRY

```
PROGRAM TRY

      INCLUDE 'DIRUSRAP.FOR'

      INTEGER IMODE,IERR,N,J,K,L
      CHARACTER*20 FILNAM,FIL2
      CHARACTER*20 PI,PII,FAKE
      INTEGER CHOICE,I,II,ITER
      DOUBLE PRECISION AVOGA
      DOUBLE PRECISION NA,STDEV,COMPO(2)
      DOUBLE PRECISION TEMP,PRESS
      DOUBLE PRECISION RADIUS,SIGMA,MOLV,CAVER
      DOUBLE PRECISION TSOL(2)
      DOUBLE PRECISION HTEMP(4),GS(4),GL(4),DG(4),DEPS

      CHOICE=2
      I=1
      II=2
      AVOGA=6.02E23
      IMODE=0
      IERR=0
      FAKE=''
      FIL2='def'
      PI='BCC_A2'
      PII='LIQUID'
      TEMP=1273.0

      CALL MTDATA_RESERVE_UNIT(12)

      OPEN(UNIT=1,FILE='input')
      READ(1,*) FILNAM
      READ(1,*) RADIUS
      READ(1,*) SIGMA
      READ(1,*) MOLV
      READ(1,*) CAVER
      READ(1,*) DEPS
      CLOSE(1)

      OPEN(UNIT=12,FILE='results')
      WRITE(12,*) "Using mpi file: ",FILNAM
      WRITE(12,*) "Melting temperature between ",PI," and ",PII
      WRITE(12,*) "For an interfacial energy of ",SIGMA," J/mol"
      WRITE(12,*) "Average composition: ",CAVER
      WRITE(12,*) "With molar volume ",MOLV," m3/mol"
      WRITE(12,*) "Gibbs energies equal within +- ",DEPS

      CALL INITIALISE_MTDATA(IMODE)
      CALL SGUMEN(1)
      CALL SGUMEN(2)
      CALL MTOPTN(IMODE,'STAGE_1=NEW')
      CALL OPEN_MPI_FILE(FILNAM,FIL2,IERR)
      CALL DISP_PHASES()
      CALL SET_PRINT_LEVEL(-2)
```

```
      DO 100 K1=0,2
         DO 110 K2=1,20

            RADIUS=5.0e-10*(10.**DBLE(K1))*DBLE(K2)

            NA=(4.*3.14159/3.)*(RADIUS**3)
            NA=NA*AVOGA/MOLV
            STDEV=DSQRT(NA*CAVER*(1.-CAVER))

            COMPO(1)=((NA*CAVER)-STDEV)/NA
            COMPO(2)=((NA*CAVER)+STDEV)/NA
            WRITE(*,*) "COMPO LOWER: ",COMPO(1)
            WRITE(*,*) "COMPO UPPER: ",COMPO(2)
            PRESS=2.0*SIGMA*MOLV/RADIUS

            PAUSE

            DO 120 L=1,2
               ITER=0
               HTEMP(1)=273.0
               HTEMP(3)=1973.0
               CALL SET_INIT_COMPONENT_AMOUNT(I,COMPO(L))
               CALL SET_INIT_COMPONENT_AMOUNT(II,(1.-COMPO(L)))
C------------- start loop
 5             HTEMP(2)=0.5*(HTEMP(1)+HTEMP(3))
               ITER=ITER+1
               DO 10 J=1,3
                  CALL SET_TEMPERATURE(HTEMP(J))
                  CALL ONLYNORM(PI,FAKE)
                  CALL COMPUTE_EQUILIBRIUM()
                  CALL DISP_RESULT(CHOICE)
                  GS(J)=GIBBS_ENERGY_OF_PHASE(I)+PRESS
                  WRITE(*,*) "GS: ",GS(J)
                  CALL ONLYNORM(PII,FAKE)
                  CALL COMPUTE_EQUILIBRIUM()
                  CALL DISP_RESULT(CHOICE)
                  GL(J)=GIBBS_ENERGY_OF_PHASE(I)
                  WRITE(*,*) "GL: ",GL(J)
                  DG(J)=GL(J)-GS(J)
 10            CONTINUE
C------------- if sign change between first two,
C------------- select upper limit as middle
               IF (DG(2)*DG(1).LE.0.0) THEN
                  HTEMP(3)=HTEMP(2)
               ELSE
                  HTEMP(1)=HTEMP(2)
               ENDIF

               IF(DABS(DG(2)).GT.DEPS.AND.ITER.LT.5000) GOTO 5
               TSOL(L)=HTEMP(2)
 120        CONTINUE
            WRITE(12,*) RADIUS,TSOL(1),TSOL(2)
 110     CONTINUE
 100  CONTINUE

      CLOSE(12)
      END
```

```
C
**********************************************************************
*
C Subroutine ONLYNORM
C This subroutine classifies normal the phase whose names are
C passed as arguments and absent all the others.


      SUBROUTINE ONLYNORM(PI,PII)

      CHARACTER*20 PI,PII
      CHARACTER*20 PVAR
      CHARACTER*20 INIT_PHASE_NAME
      INTEGER INIT_NO_OF_PHASES

      DO 10 I=1,INIT_NO_OF_PHASES()
         PVAR=INIT_PHASE_NAME(I)

         IF (PVAR.EQ.PI .OR. PVAR.EQ.PII) THEN
            CALL SET_INIT_PHASE_CLASS(I,1)
         ELSE
            CALL SET_INIT_PHASE_CLASS(I,0)
         ENDIF
 10   CONTINUE
      END

C
**********************************************************************
C Subroutine DISP_RESULT(K)
C displays the result of the last equilibrium calculation
C argument K: 1/ mass of phases and compositions in wt%
C             2/ moles of phases and compositions in mole fraction

      SUBROUTINE DISP_RESULT(K)

      INCLUDE 'DIRUSRAP.FOR'

      INTEGER K,I,J,L,M,N


      L=ACT_NO_OF_COMPONENTS()
      WRITE(*,*) EQUIL_NO_OF_PHASES()
      WRITE(*,*)

      IF (K.EQ.1) THEN
         WRITE(*,*)'Weight and components weight fractions'
         WRITE(*,300)
         DO 10 I=1,EQUIL_NO_OF_PHASES()
            N=PHASE_PRESENT_AT_EQUILIBRIUM(I)

         IF (L.GT.5) THEN
          WRITE(*,100) ACT_PHASE_NAME(N),
     &    (ACT_COMPONENT_NAME(J), J=1,5)
          WRITE(*,200) MASS_IN_PHASE(N,2),
     &    (COMPONENT_W_OF_PHASE(J,N,2), J=1,5)
          WRITE(*,*)
         ELSE
        WRITE(*,100) ACT_PHASE_NAME(N),
     &  (ACT_COMPONENT_NAME(J), J=1,ACT_NO_OF_COMPONENTS())
        WRITE(*,200) MASS_IN_PHASE(N,2),
     &  (COMPONENT_W_OF_PHASE(J,N,2), J=1,ACT_NO_OF_COMPONENTS())
```

```
         GOTO 21
         ENDIF

         IF (L.GT.10) THEN
            WRITE(*,400) (ACT_COMPONENT_NAME(J),J=6,10)
            WRITE(*,500) (COMPONENT_W_OF_PHASE(J,N,2), J=6,10)
            WRITE(*,*)
         ELSE
            M=6
            GOTO 20
         ENDIF

         IF (L.GT.15) THEN
            WRITE(*,400) (ACT_COMPONENT_NAME(J),J=11,15)
            WRITE(*,500) (COMPONENT_W_OF_PHASE(J,N,2), J=11,15)
            WRITE(*,*)
         ELSE
            M=11
            GOTO 20
         ENDIF

20     WRITE(*,400)
     & (ACT_COMPONENT_NAME(J), J=M,ACT_NO_OF_COMPONENTS())
       WRITE(*,500)
     &  (COMPONENT_W_OF_PHASE(J,N,2), J=M,ACT_NO_OF_COMPONENTS())

21     WRITE(*,300)
       WRITE(*,*)
10       CONTINUE
      ENDIF

      IF (K.EQ.2) THEN
         WRITE(*,*)'Moles and components mole fractions'
         WRITE(*,300)
         DO 30 I=1,EQUIL_NO_OF_PHASES()
            N=PHASE_PRESENT_AT_EQUILIBRIUM(I)

         IF (L.GT.5) THEN
          WRITE(*,100) ACT_PHASE_NAME(N),
     &    (ACT_COMPONENT_NAME(J), J=1,5)
          WRITE(*,200) MOLES_OF_COMPONENTS_IN_PHASE(N,2),
     &    (COMPONENT_X_OF_PHASE(J,N,2), J=1,5)
          WRITE(*,*)
         ELSE
          WRITE(*,100) ACT_PHASE_NAME(N),
     &    (ACT_COMPONENT_NAME(J), J=1,ACT_NO_OF_COMPONENTS())
          WRITE(*,200) MOLES_OF_COMPONENTS_IN_PHASE(N,2),
     &   (COMPONENT_X_OF_PHASE(J,N,2), J=1,ACT_NO_OF_COMPONENTS())
          GOTO 41
         ENDIF

         IF (L.GT.10) THEN
            WRITE(*,400) (ACT_COMPONENT_NAME(J),J=6,10)
            WRITE(*,500) (COMPONENT_X_OF_PHASE(J,N,2), J=6,10)
            WRITE(*,*)
         ELSE
            M=6
            GOTO 40
         ENDIF

         IF (L.GT.15) THEN
```

```
            WRITE(*,400) (ACT_COMPONENT_NAME(J),J=11,15)
            WRITE(*,500) (COMPONENT_X_OF_PHASE(J,N,2), J=11,15)
            WRITE(*,*)
         ELSE
            M=11
            GOTO 40
         ENDIF

 40      WRITE(*,400)
     &   (ACT_COMPONENT_NAME(J), J=M,ACT_NO_OF_COMPONENTS())
         WRITE(*,500)
     &   (COMPONENT_X_OF_PHASE(J,N,2), J=M,ACT_NO_OF_COMPONENTS())

 41      WRITE(*,300)
         WRITE(*,*)

 30      CONTINUE
      ENDIF

 100  FORMAT (1X,A,1X,5(5X,A,4X))
 200  FORMAT (E11.6,1X,5(1X,F9.7,1X))
 300  FORMAT (66('-'))
 400  FORMAT (12X,5(5X,A,4X))
 500  FORMAT (12X,5(1X,F9.7,1X))

      END


C ****************************************************************
C Subroutine DISP_COMPONENTS
C argument CHOICE: 1 / name of initial components
C                  2 / mass of initial components
C                  3 / moles of initial components
C                  4 / name of active components (after eq calc only)

      SUBROUTINE DISP_COMPONENTS(CHOICE)

      INTEGER CHOICE

      DOUBLE PRECISION INIT_COMPONENT_MASS
      DOUBLE PRECISION INIT_COMPONENT_MOLES
      INTEGER ACT_NO_OF_COMPONENTS
      CHARACTER*20 INIT_COMPONENT_NAME,ACT_COMPONENT_NAME

      WRITE(*,*)

      IF (CHOICE.EQ.1) THEN
      DO 10 I=1,INIT_NO_OF_COMPONENTS()
         WRITE(*,100) 'Component',I,'is',INIT_COMPONENT_NAME(I)
 10   CONTINUE
      ENDIF

      IF (CHOICE.EQ.2) THEN
      DO 20 I=1,INIT_NO_OF_COMPONENTS()
       WRITE(*,150) INIT_COMPONENT_NAME(I),' mass: ',
     & INIT_COMPONENT_MASS(I)
 20   CONTINUE
      ENDIF

      IF(CHOICE.EQ.3) THEN
         DO 30 I=1,INIT_NO_OF_COMPONENTS()
```

```
            WRITE(*,200) 'Component',I,'amount is',
     &      INIT_COMPONENT_MOLES(I)
 30      CONTINUE
       ENDIF

       IF (CHOICE.EQ.4) THEN
          DO 40 I=1,ACT_NO_OF_COMPONENTS()
             WRITE(*,100) 'Active Component', I, 'is',
     &       ACT_COMPONENT_NAME(I)
 40          CONTINUE
       ENDIF

 100   FORMAT (10X,A,1X,I2,1X,A,1X,A)
 150   FORMAT (10X,A,1X,A,1X,F7.4)
 200   FORMAT (10X,A,1X,I2,1X,A,1X,F7.4)
       END



C ***************************************************************
C Subroutine DISP_PHASES
C display the different phases loaded with the mpi file and their
C current status


       SUBROUTINE DISP_PHASES()
       CHARACTER*20 INIT_PHASE_NAME
       CHARACTER*6 ANSW

       LOGICAL NORMAL_INIT_PHASE

       WRITE(*,*)
       DO 10 I=1,INIT_NO_OF_PHASES()
          IF (NORMAL_INIT_PHASE(I)) THEN
             ANSW='normal'
             ELSE
             ANSW='absent'
          ENDIF
          WRITE(*,100) 'The phase',INIT_PHASE_NAME(I),'is', ANSW
 10    CONTINUE
 100   FORMAT (A,1X,A,1X,A,1X,A)
       END
```

Abstract

This project involved calculations of the melting temperatures of metallic particles of different shape, size, crystal structure and chemical composition. Such particles are now a frequent occurrence in the manufacture of carbon nanotubes. Pure iron particles were studied in the first instance, after which a second round of calculations was performed on a 10-wt% nickel-iron alloy. Both spherical and infinite cylindrical shaped particles were used, with varying radii. The properties were studied as a function of interfacial energy in the range 0.1 to 1.0 Jm^{-2}. Results obtained from these calculations revealed that spherical particles had the lowest melting temperatures. Also, reducing the particle radius and maximising the interfacial energy, maximises temperature reduction. The results were similar for both iron and the nickel-iron alloy but the change in temperature was certainly less in the alloy. As far as composition was concerned, in iron the austenite crystals had lower melting temperatures than the ferrite crystals, yet in the alloy this trend was reversed.

A statistical analysis of composition and melting temperature for a sample of 10-wt% nickel-iron alloy revealed that the statistical variation of particle composition only has a significant effect on melting temperature at extremely small radii.